Arabian Journal of Chemistry (2023) **16**, 104792

King Saud University

Arabian Journal of Chemistry

www.ksu.edu.sa
www.sciencedirect.com

ORIGINAL ARTICLE

Methylene diisocyanate - aided tailoring of nanotitania for dispersion engineering through polyurethane mixed matrix membranes: Experimental investigations

Iman Salahshoori [a], Morteza Asghari [b,c,*], Majid Namayandeh Jorabchi [d,*], Sebastian Wohlrab [d], Mehrdad Rabiei [b], Mojtaba Raji [b], Morteza Afsari [e]

[a] *Department of Chemical Engineering, Islamic Azad University, Science and Research Branch, Tehran, Iran*
[b] *Separation Processes Research Group (SPRG), Department of Chemical Engineering, University of Science and Technology of Mazandaran, Behshahr, Mazandaran, Iran*
[c] *UNESCO Chair on Coastal Geo-Hazard Analysis, Tehran, Iran*
[d] *Leibniz Institute for Catalysis, Albert-Einstein-Straße 29a, D-18059 Rostock, Germany*
[e] *Centre for Technology in Water and Wastewater, School of Civil and Environmental Engineering, University of Technology Sydney, Australia*

Received 25 September 2022; accepted 5 March 2023
Available online 11 March 2023

KEYWORDS

Carbon capture;
Environmental pooltants;
Gas separation;
Mixed Matrix Membranes;
Methylene diisocyanate (MDI)-modified (TiO_2);
Polyurethane

Abstract The present focus of environmental science is centred on addressing the significant and controversial challenge of separating acid gases. As a result, scientists are actively engaged in developing high-performance membranes that can effectively transport gases. An important factor in achieving superior gas separation efficiency is the ability to control the rate of chemical component penetration through the membrane. This has led to an increasing interest in mixed matrix membranes (MMMs) that contain inorganic nanoparticles homogeneously dispersed within the polymer matrix, which are becoming a popular alternative to traditional polymeric membranes. In this work, the morphological properties of polyurethane (PU) membrane treated with titanium dioxide (TiO_2), which is functionalized with methylene diisocyanate (MDI), were studied, and its gas transport properties, like selectivity and permeability, were evaluated. FTIR, XRD, TG, DTG, and SEM analyses were performed for neat and MMMs to study their morphological properties in phase I of the research. Our results showed that MDI modification improved the dispersion of TiO_2 in

* Corresponding authors.
E-mail addresses: asghari@mazust.ac.ir (M. Asghari), asgharimore@gmail.com, majid.jorabchi@catalysis.de (M. Namayandeh Jorabchi).
Peer review under responsibility of King Saud University.

Production and hosting by Elsevier

https://doi.org/10.1016/j.arabjc.2023.104792

the PU matrix, resulting in a more uniform and compact membrane structure. Moreover, gas permeability results showed that incorporating up to 1 wt% of unfunctionalized and functionalized TiO_2 into the PU matrix enhanced the CO_2/N_2 selectivity by 71.69% and 78.42%, respectively. Overall, this study demonstrated the potential of MDI-aided tailoring of TiO_2 for dispersion engineering in PU MMMs, which can lead to improved gas separation performance. The findings have implications for developing advanced materials for gas separation applications, particularly in industrial processes such as natural gas purification and carbon capture.

1. Introduction

Carbon dioxide (CO2) and other greenhouse gases emitted by the oil and natural gas industry play an important role in global warming (Dong et al., 2013; Guo et al., 2019). In addition, most natural gas reservoirs contain high amounts of CO2, the removal of which is both economically and environmentally beneficial (Vinoba et al., 2017; Cheng et al., 2018). In previous studies, membrane technology has been shown to be a practical and reliable method for gas separation because it is easy to use, environmentally friendly, has low capital and operating costs, and provides a controlled penetration rate of various chemical components (Li et al., 2021; Salahshoori et al., 2021; Liu and Wang, 2017; Salahshoori et al., 2023). Recently, mixed matrix membranes (MMM) have emerged as versatile and crucial membranes to overcome the limitations of conventional membranes such as polymeric membranes (impermeability and simultaneous gas selectivity) and inorganic membranes (lack of large-scale production due to high manufacturing costs) (Semsarzadeh et al., 2007; Li et al., 2022; Sadeghi et al., 2011; Hassanajili et al., 2013; Semsarzadeh et al., 2014; Amedi and Aghajani, 2016; Sodeifian et al., 2019).

It is crucial to select the applicable parent polymer and filler with suitable physical and chemical properties when attempting to create miscible blends for the final MMMs with steady performance and stable thermal and mechanical properties (Dong et al., 2013; Guo et al., 2019; Vinoba et al., 2017; Cheng et al., 2018; Li et al., 2021; Salahshoori et al., 2021). Polyurethane (PU) polymers are rubber-based polymers with a high ability to separate CO_2 from gas streams (Liu and Wang, 2017; Salahshoori et al., 2023). PU is a versatile chemical compound in terms of its structure and properties, which consists of two main segments: a soft one (polyester/polyester, associated with gas penetration) and a hard one (urea/urethane, related to mechanical strength) (Semsarzadeh et al., 2007; Li et al., 2022). There are extensive published research on the use of PU in the construction of MMMs for gas separation (Sadeghi et al., 2011; Hassanajili et al., 2013; Semsarzadeh et al., 2014; Amedi and Aghajani, 2016; Sodeifian et al., 2019).

Overall, the combination of high selectivity, tunable properties, high mechanical strength, easy production, and compatibility with other materials makes PU a suitable candidate for CO_2 gas separation membranes. These membranes have the potential to reduce the concentration of CO_2 in industrial gas streams, which can help mitigate the environmental impact of greenhouse gas emissions (Isfahani et al., 2016; Mozaffari et al., 2017; Talakesh et al., 2012; Ghadimi et al., 2019; Fakhar et al., 2019; Mansouri et al., 2021; Shoukat et al., 2022; Norouzi et al., 2022). Moreover, PU MMMs have shown significant advantages over traditional polymer membranes in gas separation due to their improved selectivity, enhanced permeability, increased stability, easy processing, and versatility. These advantages make PU MMMs promising membranes for gas separation with potential applications in various industries such as petrochemical, food and beverage, and pharmaceutical (Sodeifian et al., 2019; Maleh et al., 2022; Rayekan Iranagh et al., 2020; Ahmad et al., 2022; Norouzi et al., 2022; Sazanova et al., 2022; Rosenthal et al., 2022; Ghalei et al., 2019; Hong et al., 2022; Pacheco et al., 2021; Torre-Celeizabal et al., 2022; Fakhar et al., 2020).

In addition to parent polymers, nanoparticles (fillers) contribute significantly to MMMs' performance depending on their physicochemical properties, structure, and surface chemistry (Muntha et al., 2017; Kardani et al., 2018). There are several well-known and practical fillers that are employed for the construction of MMMs, including zeolite imidazole frameworks (ZIFs) (Guan et al., 2020; van Essen et al., 2021), metal–organic frameworks (MOFs) (Lin et al., 2018; Thür et al., 2021; Fan et al., 2018; Zhao et al., 2021), carbon nanotubes (CNTs) (Ismail et al., 2009; Park et al., 2016; Sianipar et al., 2017), zeolites (Zagho et al., 2021; Bastani et al., 2013); graphene oxide (GO) (Zhang et al., 2019; Dong et al., 2016), and mesoporous nanoparticles (Wang et al., 2020). Mesoporous fillers such as silica (SiO_2) (Nematollahi et al., 2019; Salahshoori et al., 2021), Nickel oxide (NiO) (Aframehr et al., 2020), titanium oxide (TiO_2) (Ahmad and Hågg, 2013), etc., have found widespread application in gas separation membranes synthesize due to the high gas porosity and permeability, simplicity of manufacture, and favourable pore structure. Based on published research, it has been shown that TiO_2 nanoparticles enhanced the MMMs' performance (Zhu et al., 2019; Wang et al., 2017).

It is widely acknowledged that the functionalization of TiO_2 with organic ligands and functional groups is highly effective in improving MMMs' performance (Shamsabadi et al., 2017; Xin et al., 2014). Nanoparticles are highly prone to aggregation in polymer matrixes because of their high surface energy. However, the homogeneous distribution of nanoparticles within the polymer matrix is vital for polymer nanocomposites (Ashraf et al., 2018). There is often a difference in polarity between polymer matrices and inorganic nanoparticles. It is important to note that polymers tend to be organophilic, while nanoparticles are hydrophilic. Therefore, the nanoparticles' surface must be modified to achieve maximum homogeneity and homogenous dispersion in the matrix (Hanemann and Szabó, 2010). 4,40-methylene diphenyl diisocyanate (MDI) is considered one of the most extensively applied chain extenders in the two-component systems that utilize reactive polyurethane chemistry since it comprises two isocyanate groups, and it is exceptionally reactive to hydroxyl and carboxyl groups (xxxx; Pan et al., 2018). Moreover, MDI-modified TiO_2 is pivotal and a functional inorganic filler that improves the MMMs' performance owing to the high stability, easy processing, cost-effectiveness, and improved mechanical, interoperability and thermal stability.

The main aim of this research was to synthesize state-of-the-art mixed matrix membranes (MMMs) with improved functionality employing the phase inversion method. To do this, neat TiO_2 and TiO_2 nanoparticles modified with MDI groups were synthesized and grafted with different loading ratios to the PU membrane. Then the morphology and ability of the synthesized membranes to separate carbon dioxide, methane, and nitrogen gases across various pressures were investigated.

2. Materials and methods

2.1. Materials

Commercial polyurethane (Italy, A6505, Polyester urethane, density; 1.17 g/cm^3 and Hardness; A° 65) was purchased from

Apilon Company. Dimethylformamide (DMF, Merck) has been supplied as a polymer solvent. 4,40-methylene diphenyl diisocyanate (MDI) was purchased from Merck, and nano TiO_2 (~21 nm, specific surface area: ~ 35–65 m^2/g) as filler was provided from Notrino Co. (Iran).

2.2. Procedure for preparing the membrane

As schematically depicted in Fig. 1, the phase inversion method was utilized to assemble neat membranes. The fundamental methodology behind the production of the majority of commercially available membranes is the phase inversion process. This process involves the controlled transformation of a thermodynamically stable polymer solution from a liquid state to a solid state. By using phase inversion, it is possible to create finely dispersed droplets in a continuous phase, whereas other methods like emulsion preparation, which involves dissolving surfactant in the continuous phase and adding dispersed phase with appropriate agitation, often result in unstable macroemulsions (Kumar et al., 2015).

In this way, the polymer was added to DMF solvent to yield a concentration of 8 wt%. A shaking water bath is then used to stir the solution at 60 °C and 250–300 rpm for 24 h until the polymer is completely dissolved. A 30-minute ultrasonic bath at 45 °C is used to remove the bubbles from the solution. Dope casting was done into a petri dish and subsequently placed for 24 h in an oven (Memmert, Germany) at 70 °C for solvent removal (Sadeghi et al., 2011) (Fig. 1a). The oven was also used to dry the nanoparticles in order to eliminate moisture prior to the functionalization process. After that, ~3 g of methylene diisocyanate was dissolved in ~ 25 ml of dry toluene in a 100 cc three-neck balloon. Then ~ 1 g of nano-titania was incorporated into the solution and stirred for 6 h at 60 °C under constant nitrogen reflux. Finally, to remove excess methylene diisocyanate from the solution, it was washed with dry toluene and then accommodated in an oven at 120 °C for 2 h to dry (Behniafar et al., 2015) (Fig. 1b).

In order to construct MMMs, first, Nanotitania was added to DMF, and then the solution was sonicated for 20 min in an ultrasonic for proper dispersion. Following that, 10% by weight of polyurethane was poured into the solution. A water bath was then used to stir the solution at 60° C and 300 rpm for 2 h. The remaining polymer was dissolved for at least 20 h under the same conditions as the previous step. Finally, the degassed mixture was poured onto a petri dish and transferred to the oven for 24 h to complete the phase inversion process (Fig. 1c). The fabricated membranes have been listed in Table 1.

2.3. Membranes gas transmission measurement

The method employed for measuring gas transmission through the membrane in this work is akin to the one used in our prior study (Amirkhani et al., 2020). The schematic representation of the laboratory set-up for measuring gas permeability is presented in Fig. 2. This set-up was used to conduct experiments under different pressure conditions (4–10 bar), and the measurements were used to assess the MMMs performance. The cell holder shown in Fig. 2 is located in an incubator in order to maintain a constant temperature.

The cell was composed of two polished plates with a thickness of 20 mm, which were made of stainless steel 316, 80 mm, and 180 mm internal and external diameters, respectively, and a 5 mm split between the plates occupied with plexiglass and the membrane. Further information about the parts of the cell holder is also included in Fig. 2.

A magnetic flow meter (MFM) is used to measure the permeated gas (membrane output), which is coupled to gas chromatography (GC). Gases such as CO_2, CH_4, and N_2 were passed through a membrane module which was connected to regulated-pressure cylinders to control the pressure. Equation (1) could be used to calculate the permeability of a membrane at a steady state.

$$P_A = 10^{-10} \times \frac{T_0}{T} \times \frac{P}{P_0} \times \frac{Q \times L}{A \Delta P} \quad (1)$$

here P_A stands for component A permeability (Barrer), T and T_0 denote the temperature of the incubator (K) and the standard temperature (K), respectively, P and P_0 represent the ambient and standard pressures (cmHg), Δp indicates the difference between the membrane pressure upstream and downstream, L signifies the thickness of the membranes (μm), Q (STP) refers to the permeate gas volume flow rate via the membrane (cm^3/s), and A epitomizes the membrane effective cross-sectional area (cm^2).

2.4. Membrane characterization

Fourier transform infrared spectroscopy (FTIR) was used to study the chemical structures and functional groups of the pure and the MMMs (NICOLET Magna IR 550), in the range between 400 and 4000 cm-1. First, the samples had to be placed in a vacuum oven with KBr heated to 110 °C for at least two hours to remove the moisture absorbed by the models. X-ray diffraction patterns (Philips X'pert pro MPD, Netherlands) were used to determine the crystallinity of the membrane. For all X-ray patterns (θ2), copper radiation at 40 kV voltage and 40 mA was used to produce a diffraction pattern from 10° to 80°. The surface morphology, type of particle aggregation, shape and average particle size were studied by scanning electron microscopy (SEM) (EM3200, KYKY). To avoid the destruction of the cross-sectional structure, the surface of the samples was coated with a thin layer of gold metal after being broken in liquid nitrogen and the cross-section was deposited. The thermal stability of the MMMs formed with TiO2 and MDI-TiO2 was investigated by TG analysis (Mettler Toledo, model SDTA851e) using nitrogen as atmosphere with a heating rate of 10 °C per minute.

3. Results and discussions

3.1. Characterization

3.1.1. FTIR analysis

FTIR spectra can be used to evaluate molecular interactions in blends and the changes that occur over time during such interactions (Sodeifian et al., 2019; Valizadeh et al., 2022). One of the most visible effects of FTIR in molecular interactions in PU is the intensity of the formation of hydrogen bonds between the polymer segments. Fig. 3a describes the FTIR spectra of (un)functionalized TiO_2 and MDI. According to

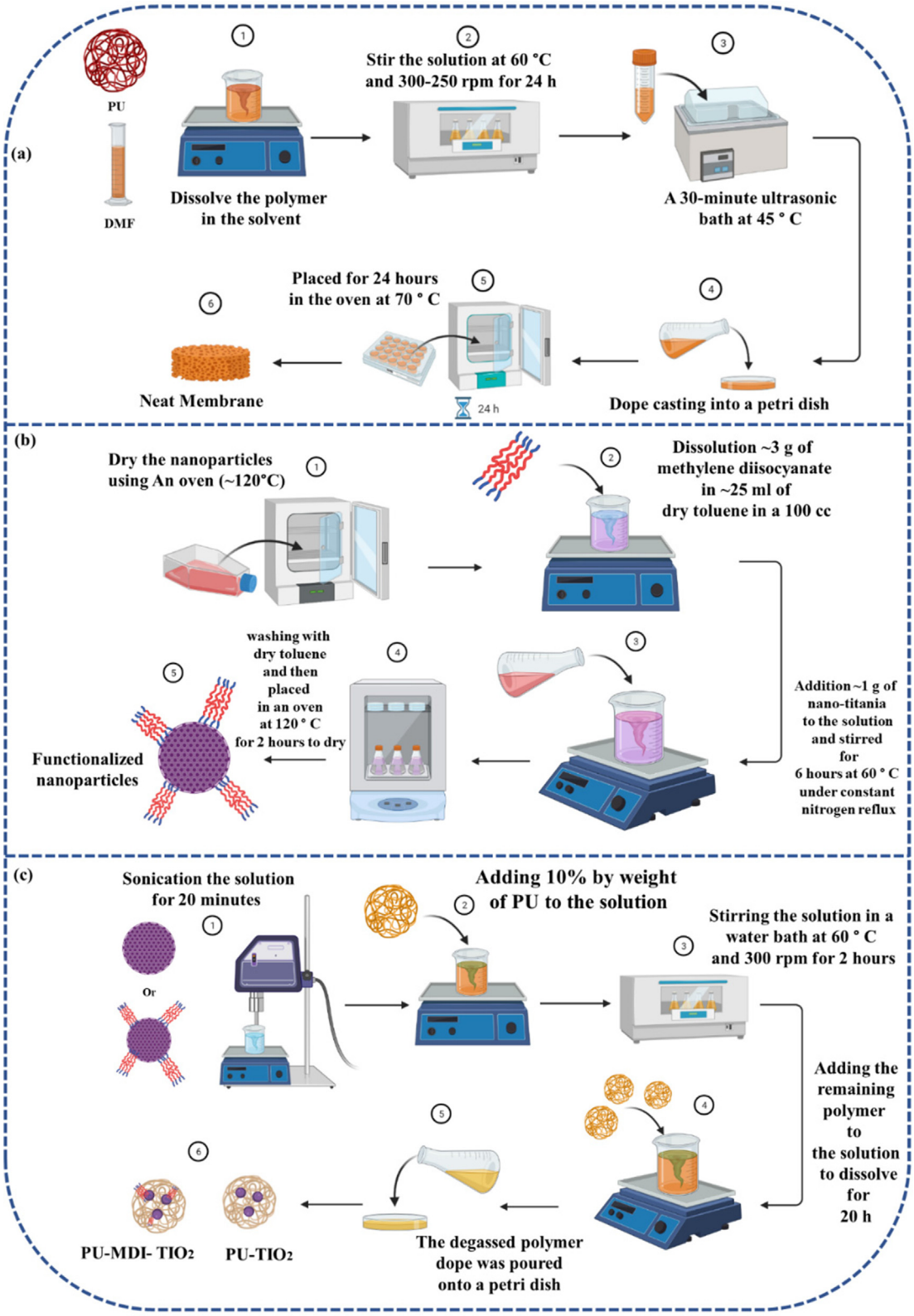

Fig. 1 A graphical representation of the neat and MMMs synthesis processes (Created with BioRender.com).

these findings, the MDI-relevant functional groups appear on the surface of nanoparticles after TiO_2 has been modified. According to Fig. 3a, the appearing peaks at wavelengths less than 800 cm^{-1} are related to Ti-O-Ti bonds. After the functionalization of nanoparticles, this peak has become smaller and thinner due to the changing in the functional group of the nano TiO_2. Furthermore, the peaks appearing in the range

Table 1 The fabricated membranes in this study.

Membrane code	Sample	Description
E-M1	PU	Neat
E-M2	PU-TiO_2/0.1	PU containing 0.1% nano-TiO_2
E-M3	PU-TiO_2/0.5	PU containing 0.5% nano-TiO_2
E-M4	PU-TiO_2/1	PU containing 1.0% nano-TiO2
E-M5	PU- TiO_2/0.1F	PU containing 0.1% functionalized nano-TiO_2
E-M6	PU-TiO_2/0.5F	PU containing 0.5% functionalized nano-TiO2
E-M7	PU-TiO_2/1F	PU containing 1.0% functionalized nano-TiO2

of 1170 cm^{-1} to 1790 cm^{-1} indicate that the nano TiO_2 has been successfully functionalized.

Fig. 3b depicts FTIR spectrum patterns of PU neat and MMMs. As revealed, the change in location and intensity of different functional groups like carbonyl (C = O), amino acid bonding (N–H), and hydrogen-bond groups is shown, which is attributed to the change in the structure of membranes. Fig. 3b indicates that carbonyl stretching vibrations of PU-MMMs offered significant information regarding the influence of TiO_2 nanoparticles on hydrogen bonds between hard and soft microphase parts of the membranes. TiO_2 nanoparticles in the MMMs led to interference in the spectra associated with the carbonyl (C = O) and amine (N–H) bonds. The frequency of absorption of carbonyl groups was indicative of how these compounds were bonded by hydrogen bonding to N–H of urethane groups. It is worth noting that if carbonyl groups connected with N–H groups of urethane, absorption of these groups appeared at lower frequencies, which is called the bonded carbonyl group. The appeared peak at higher frequencies is related to free carbonyl (Sadeghi et al., 2011). This indicates that there is free carbonyl in the polyurethane; therefore, the N–H urethane groups in the hard segment of the polyurethane are not bonded to it. Thus, the N–H group of urethane in the hard segment is hydrogen-bonded to the ester/ether group in the soft segment of the polyurethane (Sodeifian et al., 2019). The carbonyl group peaks were further investigated to survey the effect of adding nano TiO_2 on the phase separation of rigid and soft segments in the assembled membranes.

As described in Fig. 3c (magnification of the peak of carbonyl groups), adding 0.1, 0.5, and 1 wt% of TiO_2 to a polyurethane matrix leads to a decrease in the intensity of the free carbonyl peak and an increase in the intensity of the capped carbonyl peak (compared to the neat PU). These measurements revealed that more hydrogen bonds were formed between carbonyl groups of PU and the N–H groups in the hard segment, implying more phase separation had occurred (Sadeghi et al., 2011). Consequently, it can be concluded that a portion of the nanoparticles was distributed in the soft segment due to the interaction of the OH groups of TiO_2 with the ester groups of polyurethane. This resulted in a reduced hydrogen bonding between the ester groups of a soft segment

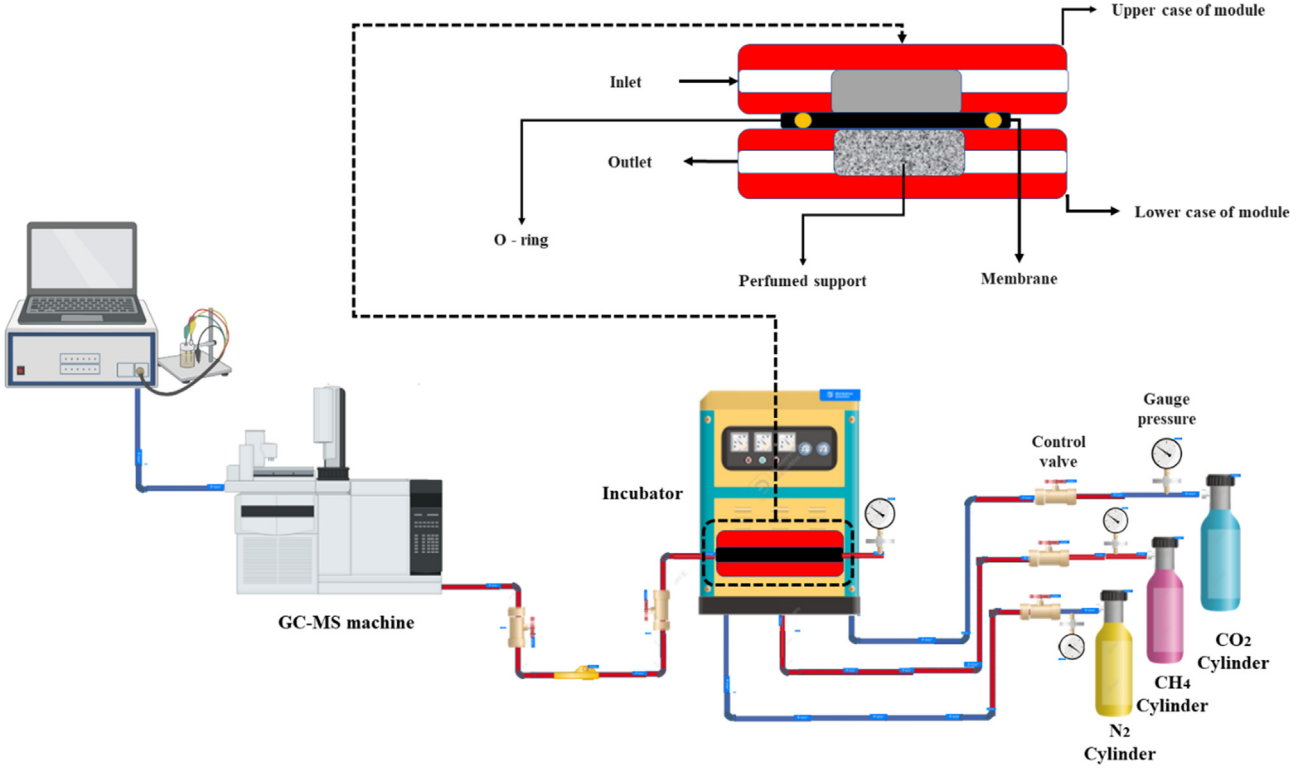

Fig. 2 A visual description of the laboratory set-up for measuring gas permeability. This image provides additional details about the membrane holder.

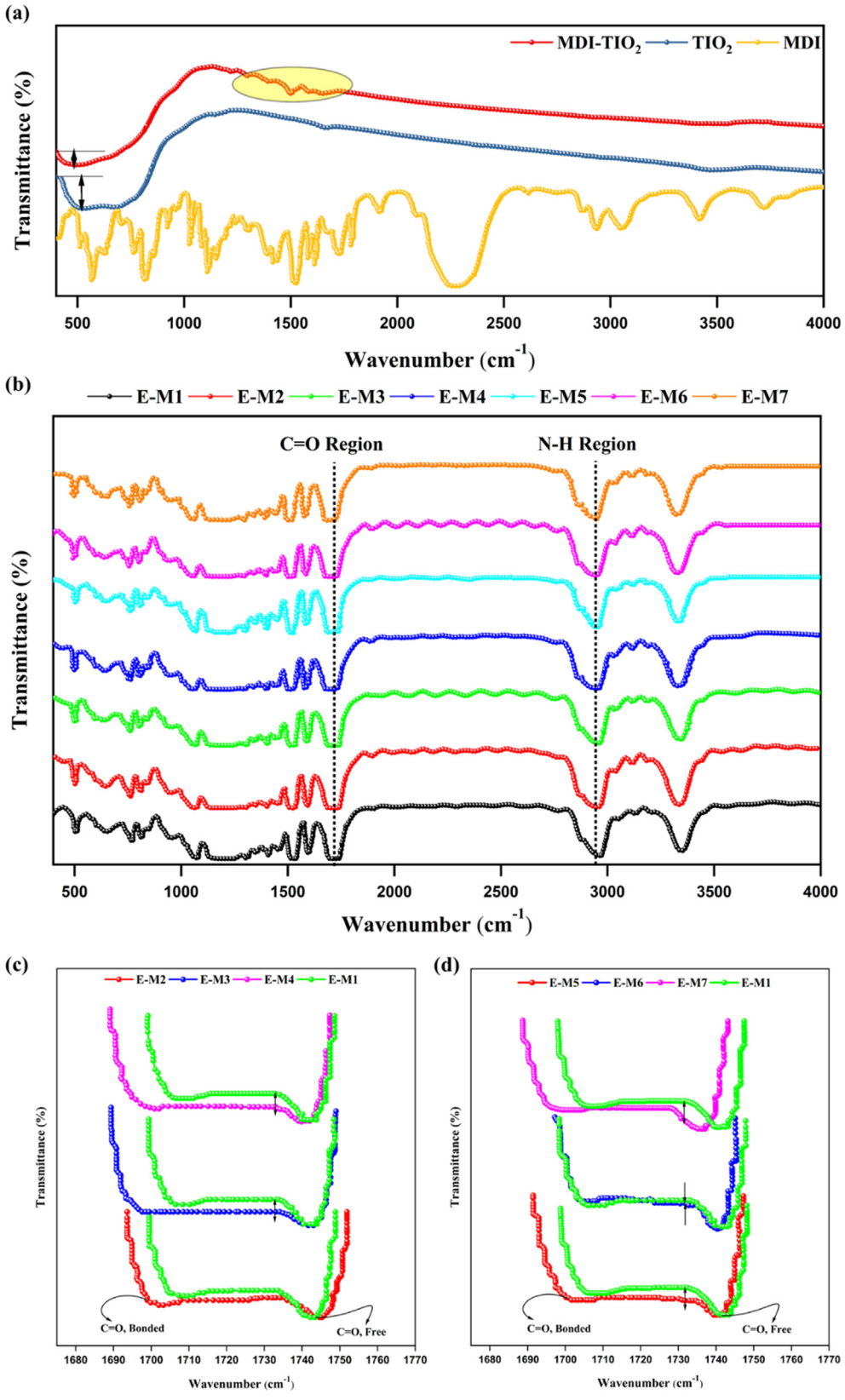

Fig. 3 FTIR spectra results of a) unfunctionalized TiO_2, functionalized TiO_2, and MDI, b) neat PU and MMMs, and Magnification of the peak of carbonyl groups related to c) PU-TIO_2 and d) PU-MDI-TIO_2.

and the N–H groups of a hard segment. Magnification of the peak of carbonyl groups for the MMMs were distinguished in Fig. 3d. As shown, the intensity of free carbonyl groups decreased with 0.1, 0.5, and 1 wt% of functionalized TiO_2 to the polyurethane membrane. Thus, MDI interactions with the membrane matrix led to a more efficient distribution of functionalized TiO_2 within soft segments. The location of the peaks associated with free and bonded carbonyls has also shifted to lower frequencies. Based on these findings, it has been demonstrated that there are more hydrogen bonds between N–H urethane groups and carbonyl urethane groups in the hard segment (Sodeifian et al., 2019). Therefore, it could be concluded that by the addition of (un)functionalized TiO_2 to the polymer matrix; the unfunctionalized TiO_2 particles interact with their OH surface groups while the functionalized TiO_2 particles interact by their OH, NH, and NCO surface groups with ester groups in the soft segment of polyurethane, resulting in more hydrogen bonds between the carbonyl groups and N–H urethane groups in the hard segment. In conclusion, based on the above elucidations, it would be reasonable to assume that both functionalized and unfunctionalized TiO_2 were distributed in the soft polymer segment.

3.1.2. X-ray diffraction analysis

An X-ray diffraction experiment was conducted to determine structural changes caused by TiO_2 and MDI-TiO_2 domains. XRD patterns of neat PU and the MMMs with 0.1, 0.5, and 1 wt% of unfunctionalized and functionalized TiO_2 are shown schematically in Fig. 4, respectively. It should be noted that the XRD patterns of polymers with large crystalline regions usually show sharp peaks and vigorous intensity, whereas those of polymers with amorphous regions are rather broad (Salahshoori et al., 2022; Salahshoori et al., 2021; Salahshoori et al., 2021). As rules, a study of the XRD results mainly depends on peak positions and intensities (Delbari et al., 2021). An analysis of the XRD pattern for neat PU membranes shows that the polymer has an amorphous structure characterized by a broad peak at approximately $2\theta = 20°$ (Sadeghi et al., 2015). Peak positions and intensity are generally related to the morphology of polyurethane membranes and the crystallinity degree within the soft and hard segments, respectively (Hassanajili et al., 2013). Fig. 4 shows that peak positions have moved toward the lower angles due to nanoparticles being added to the polymer matrix. The occurrence of interference could be a contributing factor to this phenomenon. Likewise, XRD patterns revealed that polyurethane structures had not been altered by adding (un)functionalized TiO_2. It is worth mentioning that the membrane's crystallinity significantly impacts its transport properties since gas molecules enter through its amorphous part (An adjacent crystal's space, for example) (Tan and Rodrigue, (2019) 1310.).

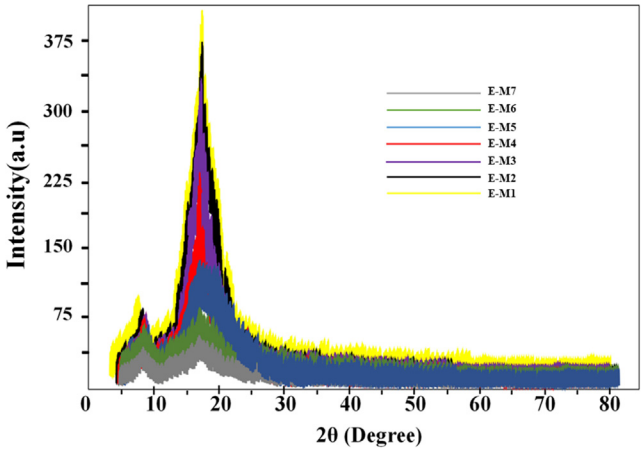

Fig. 4 An analysis of XRD patterns for polyurethane, PU neat, PU-TiO_2, and PU–MDI-TiO_2 MMMs.

The position of the PU peak was slightly changed when TiO_2 and MDI-TiO_2 particles were mixed with PU polymer, however the intensity of the peak decreased as a result of the mixing. PU peak intensity decreased with increasing TiO_2 and MDI-TiO_2 particle content, signifying increased amorphous regions, which should have an impact on the transport properties as shown later.

3.1.3. Thermogravimetric (TG) and derivative thermogravimetric (DTG) analyses

It is generally accepted that TG analysis is the most reliable technique for determining the MMMs' thermal properties. It shows the degradation range of polymer chains at different temperatures. A visual representation of the temperature-dependent weight change is plotted in Fig. 5. Based on the TG curves (Fig. 5), it is evident that polymer chains on neat and MMMs degrade at temperatures between 230 °C and 400 °C. Further, Fig. 5 indicates that PU membranes modified with TiO_2 and MDI-TiO_2 show different thermal stability with regard to weight loss (percentage), and PU-MDI-TiO_2 MMMs show higher thermal stability. As well as that, it has also been possible to identify the temperature of the degradation, the loss in weight, as well as the quantity of ash remaining in the neat and MMMs based on TG curve analysis. Fig. 5 illustrates that the MMMs samples exhibited more excellent thermal stability than neat PU samples. There were two stages in the thermal decomposition of neat PU, as shown in the TG thermogram (Fig. 5). Initially, a slight weight loss was observed between 270 °C and 320 °C; additionally, a significant weight loss was observed between 350 °C and 460 °C, suggesting that the polymer backbones were being destroyed. 98% of the membrane's weight is decomposed in the second stage, and approximately 1.5% remains in the ash state after the test. A more significant phenomenon in MMMs is the increase in ash remaining after the degradation process. As shown in Fig. 5, with the rise in the amount of TiO_2 and MDI-TiO_2 nanoparticles in the PU structure from 0.5% to 1.5%, the remaining ash has increased from 7.7% to 19.6% and 22.3% to 33.4%, respectively. This rise is indispensable in specifying the thermal stability of membranes modified with TiO_2 and MDI-TiO_2 particles as suitable fillers. The thermal stability of MMM is affected by particle inclusions in the polymer. Particles interact with polymers through their intrinsic thermal stability or their interaction level. This leads to improved MMM thermal stability because of the motion restriction of polymer chains, especially when effective interactions are present (Meshkat et al., 2018).

A thermogram with a close-spaced weight versus temperature peaks is analyzed with derivative thermogravimetry (DTG) analysis by plotting the rate of material weight change against temperature. An indication of thermal stability is pro-

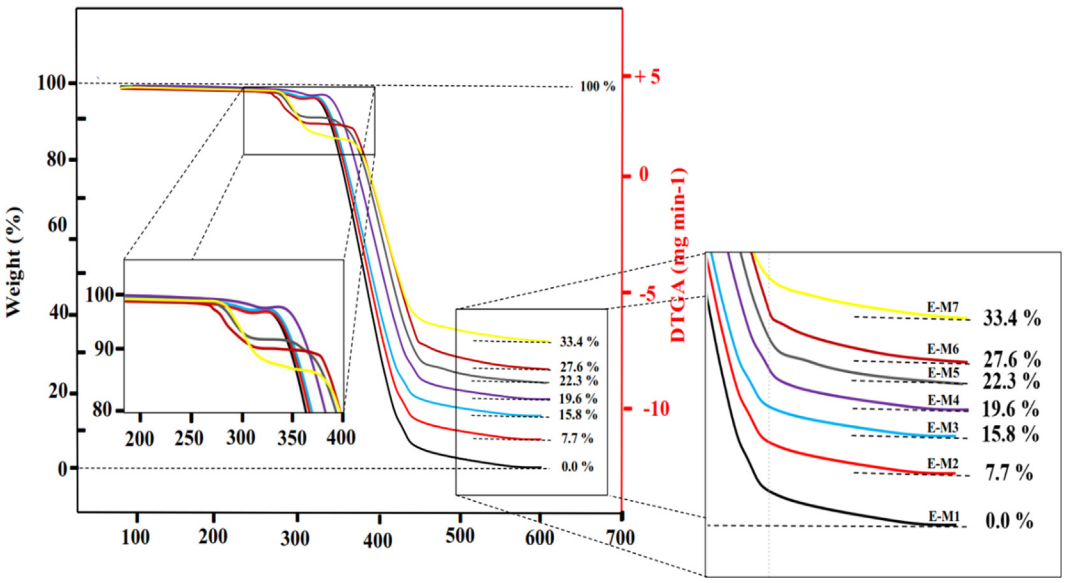

Fig. 5 A graphic representation of TG curves analysis for PU polymer chain modification with TiO_2 and MDI-TiO_2.

vided by the maximum DTG peak, which indicates the temperature at which the greatest rate of weight loss occurs. From Fig. 6, it can be seen that the main decomposition step occurs at lower temperatures with the addition of PU/TiO_2 and PU/MDI-TiO_2 MMM as the peak intensity shifts downward.

Minor defects at the polymer-MDI-TiO_2 interface are likely to be responsible for this slight decrease in thermal stability. Nevertheless, low temperature gas separations can still be carried out with the final MMM thermal stability.

3.1.4. Morphology characterization

There is a vital role in the morphology of the distributed phase within MMMs in determining their gas permeation properties (Mohamed et al., 2022). Fig. 7 (I) and Fig. 8 (II) illustrate the surface and cross-sectional SEM images of PU-MMMs containing 0.5 wt% functionalized and unfunctionalized TiO_2. It should be noted that TiO_2 contains OH-functional groups, which are responsible for the agglomerating effect on nanoparticles. It becomes evident that the dispersion of nanoparticles in the polymeric matrix was improved by functionalizing the nanoparticle (Fig. 7 (I) and Fig. 8 (II)). After functionalization, nanoparticles and polymeric chains became easier to intermix, which, in turn, led to a better distribution of nanoparticles in polymeric chains, which could hinder agglomeration. Based on the SEM images, it could be concluded that unfunctionalized TiO_2 particles were more likely to aggregate within the polymer matrix, while functionalized TiO_2 particles tended to interact with polymer chains instead through the improved functional groups on their surface. The latter results in more homogenous MMMs.

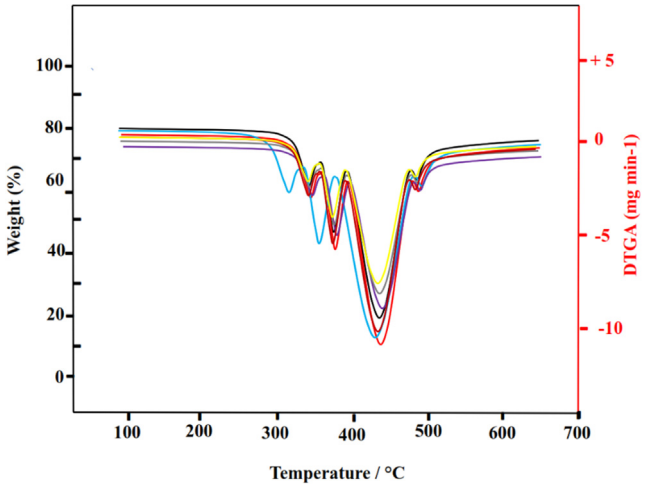

Fig. 6 A graphic representation of DTG curves analysis for PU polymer chain modification with TiO_2 and MDI-TiO_2.

3.1.5. Gas permeation results

3.1.5.1. Neat PU membranes. Permeation in PU is mainly controlled by the solution-diffusion mechanism (Isfahani et al., 2016). PU contains polar groups that make it an ideal site for adsorbing molecules (Du et al., 2012). It can be highly effective for selectively transporting CO_2 from a gas mixture. As part of the testing procedure, permeability tests were performed for pure gases (N_2, CO_2, and CH_4) to determine the membranes transport performance.

Fig. 9a demonstrates the results of the gas permeation test using a neat membrane at a pressure of up to 10 bar. As depicted in Fig. 9a, the CO_2 permeability was significantly higher compared to CH_4 and N_2. CO_2 is more permeable than CH_4 and N_2 owing to its lower kinetic diameter CO_2 (3.3 Å) than N_2 (3.88 Å) and CH_4 (3.64 Å), as well as being more polarizable and condensable (Nasirian et al., 2019; Bernardo et al., 2012) and CO_2 shows more affinity for PU as the experiment revealed. The permeation of CH_4 exhibited a higher value than that of N_2 (see Fig. 9a). A solution-diffusion mechanism can be used to describe this phenomenon (Sodeifian et al., 2019).

The dissolution of CH_4 in the polymer is more significant than of N_2. As pressure increased from 4 bar to 10 bar, the permeability for CO_2 rose from 41.34 to 59.67 barrer, but CH_4

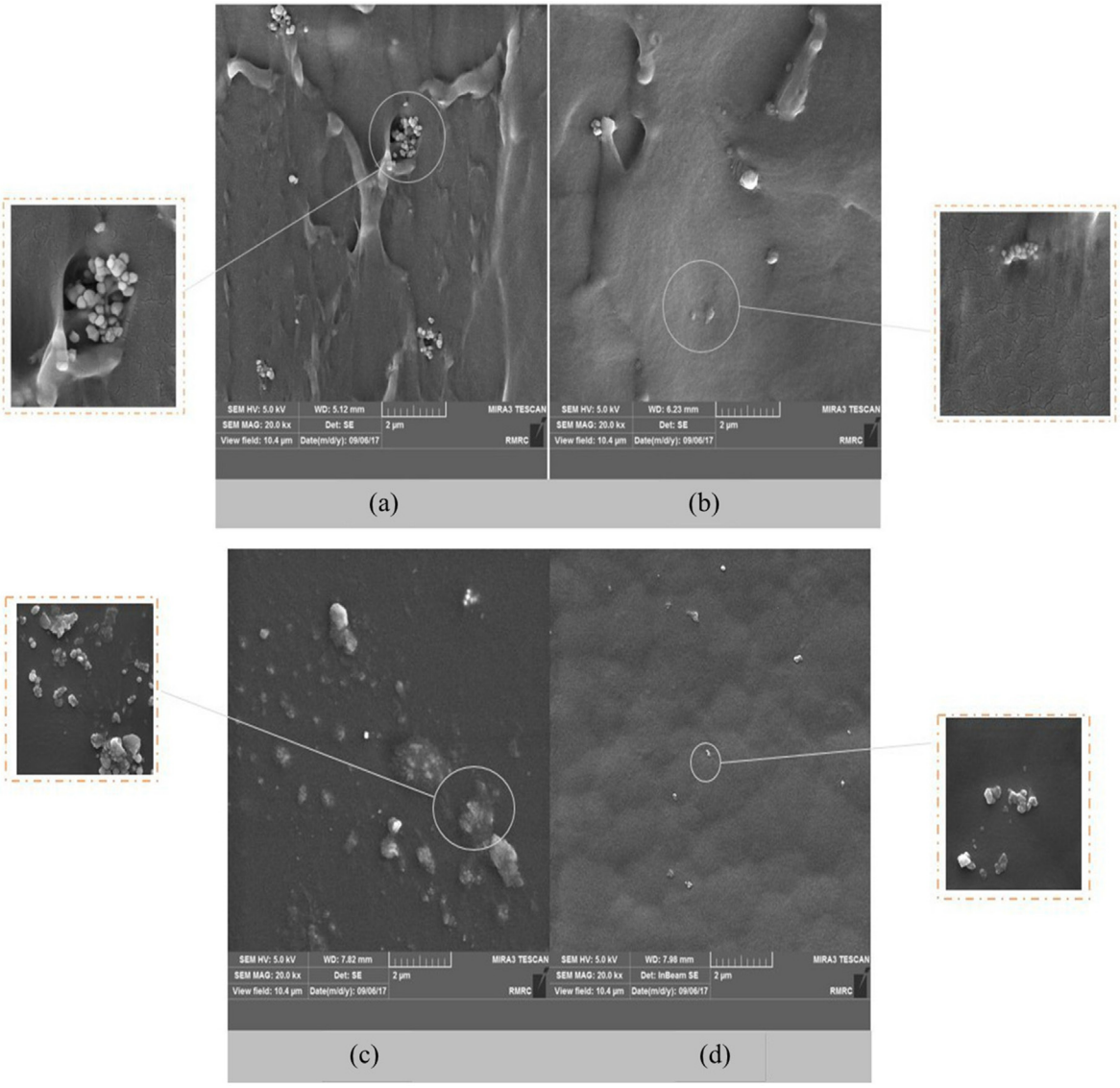

Fig. 7 SEM images of PU MMMs I) 0.5 wt% of nanoparticles. Cross-section of a) E-M3 and b) E-M6, the surface image of c) E-M3 and d) E-M6.

and N_2 permeabilities remained nearly constant. The free volume within the polymer matrix decreases as the pressure increases. In response to the reduction in the polymer-free volume, molecules with larger molecular sizes (such as N_2 and CH_4) are found to be more difficult to pass through the membrane than those with smaller molecular sizes. CO_2 molecules, in addition of being smaller in size, are more condensable under these conditions and, as a result, have a better solubility in the matrix. In addition, the phenomenon of plasticization in the polymer matrix occurs with increasing pressure in the presence of CO_2. Fig. 9b demonstrates an increase in selectivity from $\sim$ 79.2 to $\sim$ 90 for CO_2/CH_4 and $\sim$ 53 to $\sim$ 68 for CO_2/N_2 with increasing pressure from 4 to 10 bar, respectively.

3.1.5.2. Polyurethane MMMs. Fig. 9c shows the results of CO_2 permeability analysis in polyurethane membranes filled with TiO_2 and MDI-TiO_2 at a pressure of 4 bar. As demonstrated in Fig. 9c, an increase in the amount of TiO_2 leads to an initial decrease in CO_2 permeability, while the CO_2 permeability initially increases with an increase in the amount of MDI-TiO_2 in the PU membrane. As stated in the FTIR and XRD analysis sections, TiO_2 nanoparticles are distributed in the soft polyurethane section of PU-TiO_2 MMMs. In PU membranes, the soft part of the membrane that forms as a result of microphase separation is the penetrable part of the membrane for gaseous molecules. However, it is also important to note that the hard part acts as an impenetrable barrier for gas molecules because of the capability to create cross-links and change the mobility of the polymer chains, which can significantly affect the overall gas separation properties of membranes. Consequently, the distribution of TiO_2 in the soft part may decrease the mobility of the chains in the soft part and thus reduce the gas permeability by reducing the solubility of gas molecules. This may be explained by the fact that these nanoparticles have a tendency to achieve a tortuous path in the passageways of gaseous molecules when present in the soft part of the membrane. In

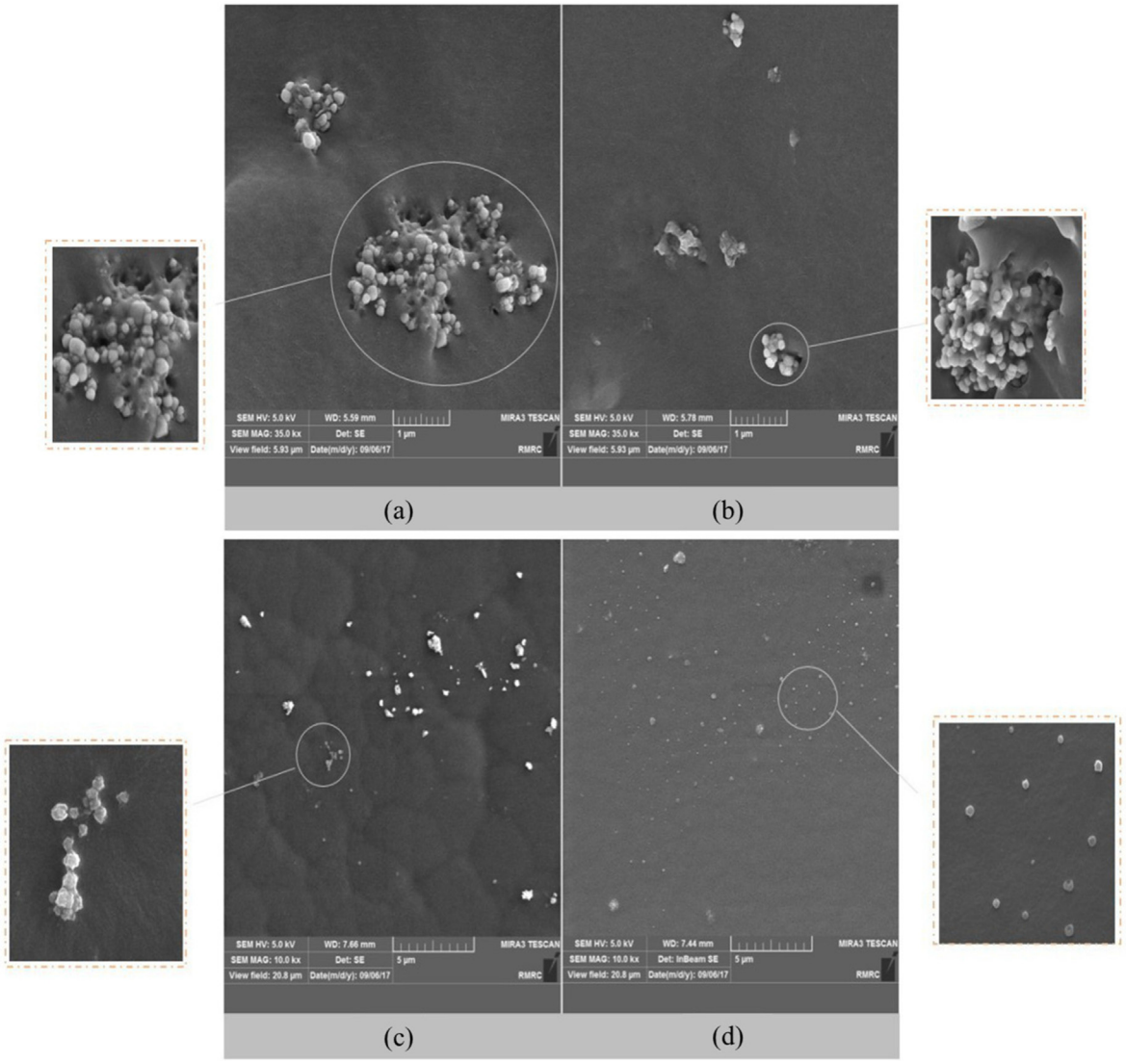

Fig. 8 SEM images of PU MMMs II) 1.0 wt% of nanoparticles. Cross-section of a) E-M4 and b) E-M7, the surface image of c) E-M4 and d) E-M7.

other words, the flexible part of polyol and soft polyurethane has sufficient mobility to pass gases, while the presence of foreign materials (nanoparticles) reduces the voids and free volume of the soft part and thus reduces the passage of gas (Chen et al., 2005). These results are consistent with Maxwell's proposed model. According to Maxwell's model, the presence of TiO_2 reduces the mobility of chains and increases the curvature of gaseous molecules passages, which reduces the permeability of the molecules in polymer matrixes. It was also observed in the XRD test results that the membrane becomes more crystalline by adding TiO_2 to the polymer matrix. Crystallized regions of the polymer structure reduce the space available for gas molecules to pass through the membrane (Wu et al., 2022; Zhang et al., 2021; Tang et al., 2023). This might also contribute to reducing the gas permeability of polymer membranes (Sadeghi et al., 2011). Based on the figure, the highest permeability is obtained at 1% TiO_2 concentration, which can be attributed to increasing polar groups of OH in the polymer matrix, which increases interactions with CO_2 molecules and ultimately leads to further adsorption and dissolution of CO_2 within the membrane matrix.

On the other hand, as shown in Fig. 9c, gas permeability is increased by adding MDI-TiO_2 with different loading into the polymer matrix. In accordance with the information provided in the FTIR and XRD test results, it is plausible to imagine the distribution of these nanoparticles in both the soft and hard parts of the polymer. The presence of nanoparticles in the hard part of the polymer results from interactions with polar groups, which can disrupt the order and polymer chains density, which then leads to a decrease in crystallinity of polymer structures by removing the strong bonds in the chain in the hard phase, which increases gas permeability and the space available for the polymer to cross the membrane. It can also be said that the distribution of a significant portion of MDI-TiO_2 in the hard part does not reduce the free volume in the soft part of the polymer (permeable part). The SEM image

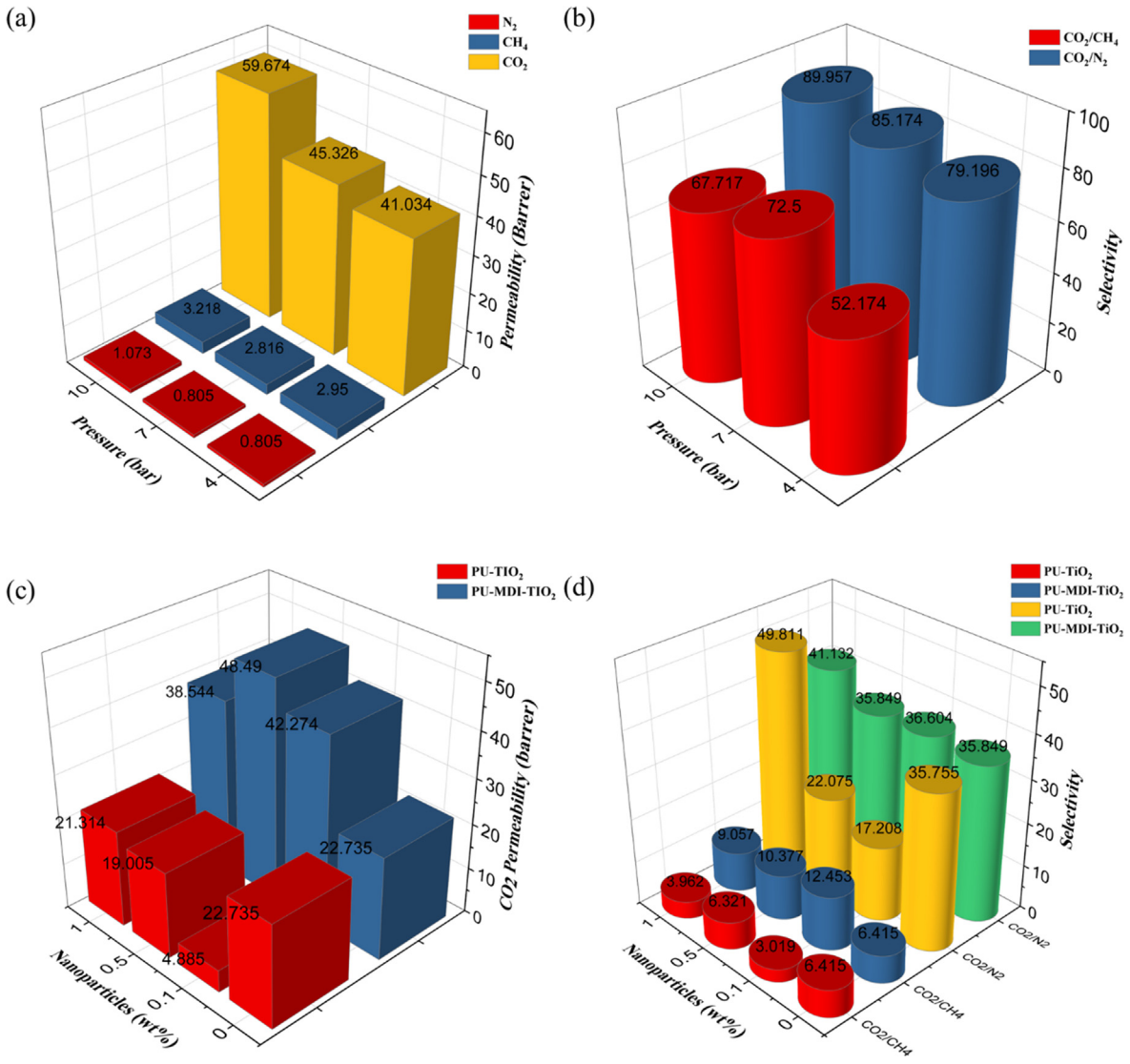

Fig. 9 Characteristics of neat PU membranes for gas permeation over pressure a) permeability of the N_2, CH_4, and CO_2, b) selectivity of the CO_2/N_2 and CO_2/CH_4, c) CO_2 permeation for PU-TiO_2 and PU-MDI-TiO_2 membrane versus nanoparticle loading and d) CO_2/CH_4 and CO_2/N_2 selectivity of PU-TiO_2 and PU-MDI-TiO_2 membrane versus nanoparticle loading.

results also indicated that MDI-TiO_2 disperses better in the polymer matrix than TiO_2, which results in improved gas separation results.

Fig. 9d shows the changes in CO_2/N_2 and CO_2/CH_4 selectivity in PU membranes at a pressure of 4 bar with increasing weight percentages of TiO_2 and MDI-TiO_2. Based on the figure, it can be observed that the CO_2/N_2 selectivity is typically elevated in comparison with that of CO_2/CH_4 across all membranes owing to the elevated CH_4 solubility and permeability in comparison with N_2 for polymer-based rubber membranes.

Based on the selectivity analysis of neat and MMMs, it was evident that the CO_2/CH_4 and CO_2/N_2 selectivity has been increased in MMMs compared to neat PU membranes. An ester group is present in the soft polymer part, where it is bonded to the hydroxyl groups on the nanoparticle surface, resulting in a reduction in the polymer chain mobility, which consequently reduces the rubber properties of PU (reduces the solubility of polarizable gases). Based on Fig. 9d, increasing the loading of nanoparticles in the membrane increases the selectivity for CO_2/N_2. This is due to the increase in the number of polar groups in the polymer substrate, resulting in increased CO_2 adsorption. The result is that larger N_2 and CH_4 molecules are more constrained to pass through the membrane than small CO_2 molecules. This leads to an increase in selectivity.

The impact of increasing pressure on the permeability of the CO_2 gas changes in neat and MMMs membranes with different loading percentages are depicted in Fig. 10a-b.

It is worth noting that increasing pressure causes molecules to penetrate into the polymer matrix deeper, which reduces the free space in the polymer matrix for gas to pass through. Moreover, molecules with larger molecular sizes (N_2 and CH_4) are more restricted from passing through the membrane than gases with smaller molecular sizes due to the reduction in the free volume of the polymer. Additionally, CO_2 molecules, in addition to being smaller in size, are more condensable and

polarizable and, as a result, are more likely to dissolve. As the polymer chain plasticization is induced by CO_2, the polymer matrix becomes more mobile, and the free volume of the polymeric chain increases, thus enhancing gas penetration.

Fig. 10c-f shows the effect of increasing pressure on the CO2/N2 and CO2/CH4 selectivity in PU membranes that have been treated with TiO_2 and MDI-TiO_2 at different loadings. With MMMs and pure polyurethane membranes, increasing the pressure would allow a higher CO_2 permeability, while virtually the same amount of permeability would be maintained for the other two gases. Therefore, the selectivity of CO_2/N_2 and CO_2/CH_4 in the PU-TiO_2 and PU-MDI-TiO_2 membranes increases with increasing gas pressure. When the effect of pressure on selectivity is compared between neat and MMM membranes, it can be concluded that the dependence of MMM membranes on pressure is less than that of neat membranes. It appears that adding nanoparticles to a polymer membrane matrix increases its rigidity and decreases the mobility of its

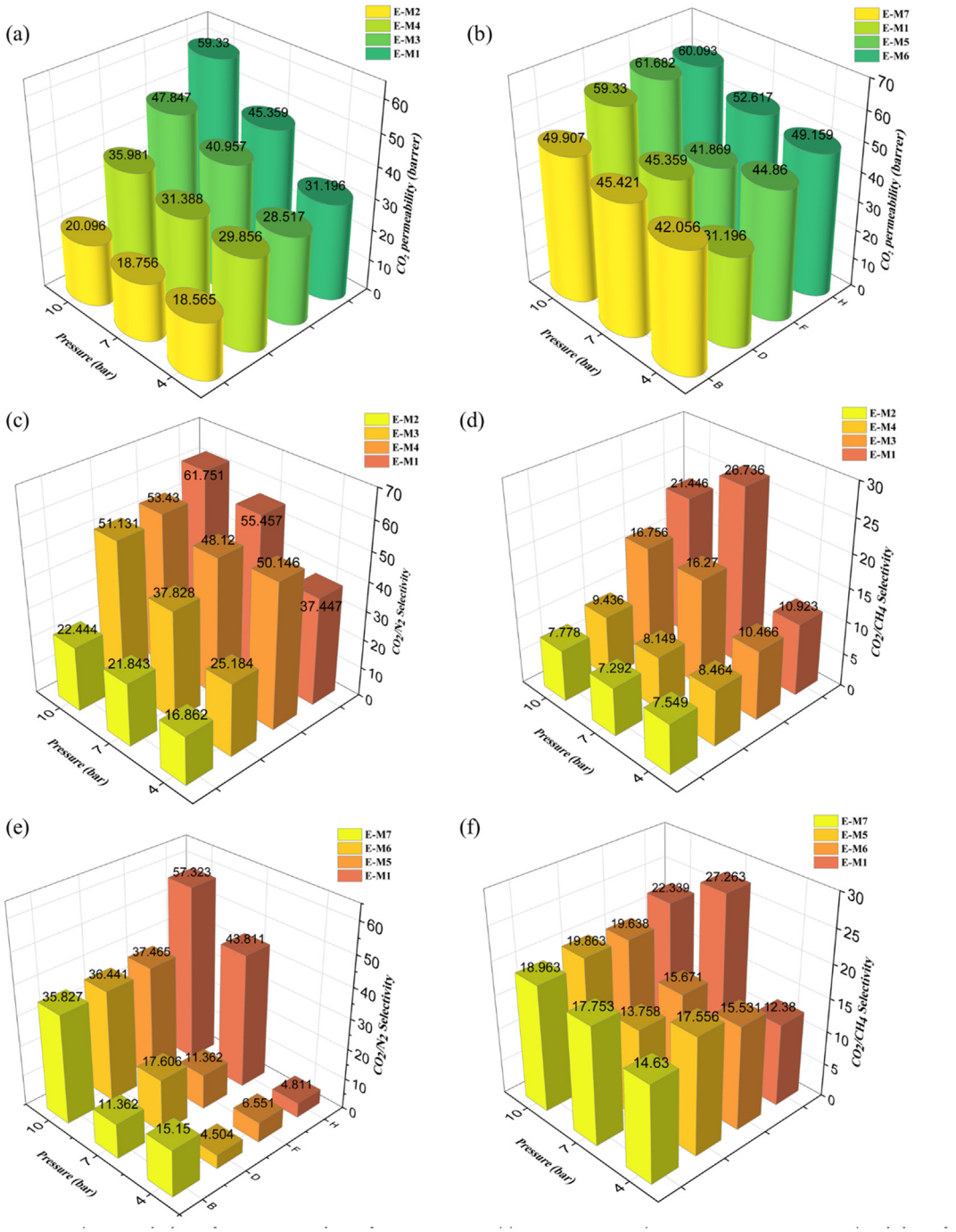

Fig. 10 Characteristics of gas permeation of a) neat PU and b) MMMs membrane versus pressure, selectivity of the c) CO_2/N_2 and d) CO_2/CH_4 in PU-TiO_2, and selectivity of the e) CO_2/N_2 and f) CO_2/CH_4 in PU-MDI-TiO_2 membrane versus pressure.

chains, reducing the membrane-free volume fraction and, as a result, increasing the pressure, has less impact on the gas permeability.

Notably, achieving good dispersion and compatibility of the nanoparticles in the polymer matrix and solid interfacial interactions between them are crucial for improving the gas separation performance of the MMMs (Zhu et al., 2016). Strategies such as surface modification of the nanoparticles, copolymerization of the nanoparticles with the polymer matrix, or optimization of the processing conditions can be used to achieve these objectives (Kamble et al., 2021). The primary results in our study demonstrated that the functionalization of TiO_2 with MDI can enhance the dispersion and compatibility of the nanoparticles in the PU matrix, leading to stronger interfacial interactions and improved gas separation performance of the synthesized mixed matrix membranes. MDI-modified TiO_2 is a type of inorganic filler that has several advantages compared to other fillers in constructing mixed matrix membranes, including:

1. **High compatibility with polymer matrices:** MDI-modified TiO_2 has a high affinity for various types of polymer matrices used in mixed matrix membranes. This makes it easier to disperse the filler within the polymer matrix, resulting in improved mechanical and transport properties.
2. **Enhanced interfacial interaction:** The modified TiO_2 particles have a reactive surface that can form covalent bonds with the polymer matrix. This enhanced interfacial interaction results in stronger adhesion between the filler and polymer, leading to improved mechanical strength and reduced filler leaching.
3. **Increased surface area:** MDI-modified TiO_2 has a high surface area, which increases the number of active sites available for interaction with the polymer matrix. This can lead to improved transport properties and increased selectivity in the mixed matrix membrane.
4. **Improved selectivity:** The high surface area of MDI-modified TiO_2 allows for the creation of a more tortuous path for gas transport in the mixed matrix membrane. This can enhance the selectivity of the membrane, making it more effective at separating gases.
5. **Enhanced thermal stability:** MDI-modified TiO_2 can improve the thermal stability of the mixed matrix membrane, making it more resistant to degradation at high temperatures.

4. Conclusion

The effect of pure TiO_2 nanoparticles and their functionalization with MDI on polyurethane membranes' morphological and transport properties has been investigated using experimental techniques. SEM, FTIR, TG, DTG and XRD analyses were utilized to characterize the fabricated neat and MMMs. Phase separation in FTIR results was observed between soft and hard segments of polyurethane filled with functionalized and (un)functionalized TiO_2. In other words, a portion of the nanoparticles were deposited in the soft segment as a result of an interaction between the OH and esters of PU. This leads to a reduction of the hydrogen bonds between the ester groups of the soft segment and the N–H groups of the hard segment. Moreover, the unfunctionalized TiO_2 by its surface OH groups and the functionalized TiO_2 through the interaction of its surface groups (OH, NH and NCO) interacted well with ester groups in the soft segment of polyurethane and distributed among the polymer chains, resulting in more hydrogen bonds between the carbonyl groups and N–H urethane groups in the hard segment. Using the SEM images, it was visible that the functionalized particles dispersed better within the polymer matrix than the unfunctionalized ones. Adding both functionalized and unfunctionalized TiO_2 improved the MMMs selectivity through gas permeation results. It can be concluded that adding functionalized TiO_2 into the polymer matrix promoted the gas permeation properties of polyurethane membranes. The structural properties as well as the permeation behaviour for single gases and mixtures therefrom, serve as the basis for simulations in further work to generate a deeper understanding of the underlying mechanisms. For future work, the effect of different nanoparticles with different functional groups to treat the PU can be studied and their effects on the morphology and gas separation ability of this membrane to separate important industrial and hazardous gases can be assessed. Blending PU with various copolymers produces innovative composites that can be studied to evaluate their morphology and gas separation enhancements in mixed matrix membranes (MMMs). Additionally, the Design of Experiment (DOE) methodology is a valuable tool that can be employed to optimize diverse parameters including temperature, pressure, concentration, and pH.

CRediT authorship contribution statement

Iman Salahshoori: Conceptualization, Methodology, Investigation, Writing – original draft. **Morteza Asghari:** Conceptualization, Methodology, Resources, Writing – review & editing, Supervision. **Majid Namayandeh Jorabchi:** Investigation, Formal analysis, Methodology. **Sebastian Wohlrab:** Resources, Writing – review & editing. **Mehrdad Rabiei:** Formal analysis, Methodology. **Mojtaba Raji:** Writing – original draft. **Morteza Afsari:** Methodology.

Declaration of Competing Interest

The authors declare that they have no known competing financial interests or personal relationships that could have appeared to influence the work reported in this paper.

References

Aframehr, W.M., Molki, B., Bagheri, R., Heidarian, P., Davodi, S.M., 2020. Characterization and enhancement of the gas separation properties of mixed matrix membranes: polyimide with nickel oxide nanoparticles. Chem. Eng. Res. Des. 153, 789–805. https://doi.org/10.1016/j.cherd.2019.11.006.

Ahmad, J., Hågg, M.B., 2013. Polyvinyl acetate/titanium dioxide nanocomposite membranes for gas separation. J. Membr. Sci. 445, 200–210. https://doi.org/10.1016/j.memsci.2013.04.052.

Ahmad, A., Sabir, A., Iqbal, S.S., Felemban, B.F., Riaz, T., Bahadar, A., Hossain, N., Khan, R.U., Inam, F., 2022. Novel antibacterial polyurethane and cellulose acetate mixed matrix membrane modified with functionalized TiO2 nanoparticles for water treatment applications. Chemosphere 301,. https://doi.org/10.1016/j.chemosphere.2022.134711 134711.

Amedi, H.R., Aghajani, M., 2016. Gas separation in mixed matrix membranes based on polyurethane containing SiO2, ZSM-5, and ZIF-8 nanoparticles. J. Nat. Gas Sci. Eng. 35, 695–702. https://doi.org/10.1016/j.jngse.2016.09.015.

Amirkhani, F., Harami, H.R., Asghari, M., 2020. CO2/CH4 mixed gas separation using poly(ether-b-amide)-ZnO nanocomposite membranes: experimental and molecular dynamics study. Polym. Test. 86,. https://doi.org/10.1016/j.polymertesting.2020.106464 106464.

Ashraf, M.A., Peng, W., Zare, Y., Rhee, K.Y., 2018. Effects of size and aggregation/agglomeration of nanoparticles on the interfacial/interphase properties and tensile strength of polymer nanocom-

posites. Nanoscale Res. Lett. 13 (1), 214. https://doi.org/10.1186/s11671-018-2624-0.

Bastani, D., Esmaeili, N., Asadollahi, M., 2013. Polymeric mixed matrix membranes containing zeolites as a filler for gas separation applications: a review. J. Ind. Eng. Chem. 19 (2), 375–393. https://doi.org/10.1016/j.jiec.2012.09.019.

Behniafar, H., Alimohammadi, M., Malekshahinezhad, K., 2015. Transparent and flexible films of new segmented polyurethane nanocomposites incorporated by NH2-functionalized TiO2 nanoparticles. Prog. Org. Coat. 88, 150–154. https://doi.org/10.1016/j.porgcoat.2015.06.030.

Bernardo, P., Jansen, J.C., Bazzarelli, F., Tasselli, F., Fuoco, A., Friess, K., Izák, P., Jarmarová, V., Kačírková, M., Clarizia, G., 2012. Gas transport properties of Pebax®/room temperature ionic liquid gel membranes. Sep. Purif. Technol. 97, 73–82. https://doi.org/10.1016/j.seppur.2012.02.041.

Chen, Y., Zhou, S., Yang, H., Wu, L., 2005. Structure and properties of polyurethane/nanosilica composites. J. Appl. Polym. Sci. 95 (5), 1032–1039.

Cheng, Y., Wang, Z., Zhao, D., 2018. Mixed matrix membranes for natural gas upgrading: current status and opportunities. Ind. Eng. Chem. Res. 57 (12), 4139–4169. https://doi.org/10.1021/acs.iecr.7b04796.

Delbari, S.A., Shakeri, M.S., Salahshoori, I., Shahedi Asl, M., Sabahi Namini, A., Abdolmaleki, A., Sheikhlou, M., Farvizi, M., Jang, H. W., Shokouhimehr, M., 2021. Characterization of TiC ceramics with SiC and/or WC additives using electron microscopy and electron probe micro-analysis. J. Taiwan Inst. Chem. Eng. 123, 245–253. https://doi.org/10.1016/j.jtice.2021.05.039.

Dong, G., Li, H., Chen, V., 2013. Challenges and opportunities for mixed-matrix membranes for gas separation. J. Mater. Chem. A 1 (15), 4610–4630. https://doi.org/10.1039/C3TA00927K.

Dong, G., Hou, J., Wang, J., Zhang, Y., Chen, V., Liu, J., 2016. Enhanced CO2/N2 separation by porous reduced graphene oxide/Pebax mixed matrix membranes. J. Membr. Sci. 520, 860–868. https://doi.org/10.1016/j.memsci.2016.08.059.

Du, N., Park, H.B., Dal-Cin, M.M., Guiver, M.D., 2012. Advances in high permeability polymeric membrane materials for CO2 separations. Energ. Environ. Sci. 5 (6), 7306–7322. https://doi.org/10.1039/C1EE02668B.

Fakhar, A., Sadeghi, M., Dinari, M., Lammertink, R., 2019. Association of hard segments in gas separation through polyurethane membranes with aromatic bulky chain extenders. J. Membr. Sci. 574, 136–146. https://doi.org/10.1016/j.memsci.2018.12.062.

Fakhar, A., Maghami, S., Sameti, E., Shekari, M., Sadeghi, M., 2020. Gas separation through polyurethane–ZnO mixed matrix membranes and mathematical modeling of the interfacial morphology. SPE Polymers 1 (2), 113–124. https://doi.org/10.1002/pls2.10023.

Fan, L., Kang, Z., Shen, Y., Wang, S., Zhao, H., Sun, H., Hu, X., Sun, H., Wang, R., Sun, D., 2018. Mixed matrix membranes based on metal-organic frameworks with tunable pore size for CO2 separation. Cryst. Growth Des. 18 (8), 4365–4371. https://doi.org/10.1021/acs.cgd.8b00307.

Ghadimi, A., Gharibi, R., Yeganeh, H., Sadatnia, B., 2019. Ionic liquid tethered PEG-based polyurethane-siloxane membranes for efficient CO2/CH4 separation. Mater. Sci. Eng. C 102, 524–535. https://doi.org/10.1016/j.msec.2019.04.057.

Ghalei, B., Isfahani, A.P., Nilouyal, S., Vakili, E., Salooki, M.K., 2019. Effect of polyvinyl alcohol modified silica particles on the physical and gas separation properties of the polyurethane mixed matrix membranes. Silicon 11 (3), 1451–1460. https://doi.org/10.1007/s12633-018-9959-0.

Guan, W., Dai, Y., Dong, C., Yang, X., Xi, Y., 2020. Zeolite imidazolate framework (ZIF)-based mixed matrix membranes for CO2 separation: a review. J. Appl. Polym. Sci. 137 (33), 48968. https://doi.org/10.1002/app.48968.

Guo, X., Qiao, Z., Liu, D., Zhong, C., 2019. Mixed-matrix membranes for CO2 separation: role of the third component. J. Mater. Chem. A 7 (43), 24738–24759. https://doi.org/10.1039/C9TA09012F.

Hanemann, T., Szabó, D.V., 2010. Polymer-nanoparticle composites: from synthesis to modern applications. Materials 3 (6). https://doi.org/10.3390/ma3063468.

Hassanajili, S., Masoudi, E., Karimi, G., Khademi, M., 2013. Mixed matrix membranes based on polyetherurethane and polyesterurethane containing silica nanoparticles for separation of CO2/CH4 gases. Sep. Purif. Technol. 116, 1–12. https://doi.org/10.1016/j.seppur.2013.05.017.

Hong, T., Li, Y., Wang, S., Li, Y., Jing, X., 2022. Polyurethane-based gas separation membranes: a review and perspectives. Sep. Purif. Technol. 301,. https://doi.org/10.1016/j.seppur.2022.122067 122067.

Isfahani, A.P., Sadeghi, M., Dehaghani, A.H.S., Aravand, M.A., 2016. Enhancement of the gas separation properties of polyurethane membrane by epoxy nanoparticles. J. Ind. Eng. Chem. 44, 67–72. https://doi.org/10.1016/j.jiec.2016.08.012.

Isfahani, A.P., Ghalei, B., Bagheri, R., Kinoshita, Y., Kitagawa, H., Sivaniah, E., Sadeghi, M., 2016. Polyurethane gas separation membranes with ethereal bonds in the hard segments. J. Membr. Sci. 513, 58–66. https://doi.org/10.1016/j.memsci.2016.04.030.

Ismail, A.F., Goh, P.S., Sanip, S.M., Aziz, M., 2009. Transport and separation properties of carbon nanotube-mixed matrix membrane. Sep. Purif. Technol. 70 (1), 12–26. https://doi.org/10.1016/j.seppur.2009.09.002.

K.B.H. Badri, W.C. Sien, M. Shahrom, L.C. Hao, N.Y. Baderuliksan, N. Norzali, FTIR spectroscopy analysis of the prepolymerization of palm-based polyurethane.

Kamble, A.R., Patel, C.M., Murthy, Z.V.P., 2021. A review on the recent advances in mixed matrix membranes for gas separation processes. Renew. Sustain. Energy Rev. 145,. https://doi.org/10.1016/j.rser.2021.111062 111062.

Kardani, R., Asghari, M., Mohammadi, T., Afsari, M., 2018. Effects of nanofillers on the characteristics and performance of PEBA-based mixed matrix membranes. Rev. Chem. Eng. 34 (6), 797–836. https://doi.org/10.1515/revce-2017-0001.

Kumar, A., Li, S., Cheng, C.-M., Lee, D., 2015. Recent developments in phase inversion emulsification. Ind. Eng. Chem. Res. 54 (34), 8375–8396. https://doi.org/10.1021/acs.iecr.5b01122.

Li, X.-Y., Li, Q.-F., Zhao, Y.-H., Kang, M.-Q., Wang, J.-W., 2022. Utilization of carbon dioxide in polyurethane. J. Fuel Chem. Technol. 50 (2), 195–209. https://doi.org/10.1016/S1872-5813(21)60145-7.

Li, S., Liu, Y., Wong, D.A., Yang, J., 2021. Recent advances in polymer-inorganic mixed matrix membranes for CO2 separation. Polymers 13 (15). https://doi.org/10.3390/polym13152539.

Lin, R., Villacorta Hernandez, B., Ge, L., Zhu, Z., 2018. Metal organic framework based mixed matrix membranes: an overview on filler/polymer interfaces. J. Mater. Chem. A 6 (2), 293–312. https://doi.org/10.1039/C7TA07294E.

Liu, S., Wang, X., 2017. Polymers from carbon dioxide: polycarbonates, polyurethanes. Curr. Opin. Green Sustain. Chem. 3, 61–66. https://doi.org/10.1016/j.cogsc.2016.08.003.

Maleh, M.S., Kiani, S., Raisi, A., 2022. Study on the advantageous effect of nano-clay and polyurethane on structure and CO2 separation performance of polyethersulfone based ternary mixed matrix membranes. Chem. Eng. Res. Des. 179, 27–40. https://doi.org/10.1016/j.cherd.2022.01.011.

Mansouri, M., Ghadimi, A., Gharibi, R., Norouzbahari, S., 2021. Gas permeation properties of highly cross-linked castor oil-based polyurethane membranes synthesized through thiol-yne click polymerization. React. Funct. Polym. 158,. https://doi.org/10.1016/j.reactfunctpolym.2020.104799 104799.

Meshkat, S., Kaliaguine, S., Rodrigue, D., 2018. Mixed matrix membranes based on amine and non-amine MIL-53(Al) in Pebax®

MH-1657 for CO2 separation. Sep. Purif. Technol. 200, 177–190. https://doi.org/10.1016/j.seppur.2018.02.038.

Mohamed, A., Yousef, S., Tonkonogovas, A., Makarevicius, V., Stankevičius, A., 2022. High performance of PES-GNs MMMs for gas separation and selectivity. Arab. J. Chem. 15, (2). https://doi.org/10.1016/j.arabjc.2021.103565 103565.

Mozaffari, V., Sadeghi, M., Fakhar, A., Khanbabaei, G., Ismail, A.F., 2017. Gas separation properties of polyurethane/poly(ether-block-amide) (PU/PEBA) blend membranes. Sep. Purif. Technol. 185, 202–214. https://doi.org/10.1016/j.seppur.2017.05.028.

Muntha, S.T., Kausar, A., Siddiq, M., 2017. A review featuring fabrication, properties, and application of polymeric mixed matrix membrane reinforced with different fillers. Polym.-Plast. Technol. Eng. 56 (18), 2043–2064. https://doi.org/10.1080/03602559.2017.1298801.

Nasirian, D., Salahshoori, I., Sadeghi, M., Rashidi, N., Hassanzadeganroudsari, M., 2019. Investigation of the gas permeability properties from polysulfone/polyethylene glycol composite membrane. Polym. Bull. https://doi.org/10.1007/s00289-019-03031-3.

Nematollahi, M.H., Babaei, S., Abedini, R., 2019. CO2 separation over light gases for nano-composite membrane comprising modified polyurethane with SiO2 nanoparticles. Korean J. Chem. Eng. 36 (5), 763–779. https://doi.org/10.1007/s11814-019-0251-9.

A.M. Norouzi, M. Elyasi Kojabad, M. Chapalaghi, A. Hosseinkhani, A. Arabloo nareh, E. Nemati Lay, Polyester-based polyurethane mixed-matrix membranes incorporating carbon nanotube-titanium oxide coupled nanohybrid for carbon dioxide capture enhancement: Molecular simulation and experimental study, Journal of Molecular Liquids 360 (2022) 119540. https://doi.org/https://doi.org/10.1016/j.molliq.2022.119540

A. Norouzi, E. Nemati Lay, A. Arabloo nareh, A. Hosseinkhani, M. Chapalaghi, Functionalized nanodiamonds in polyurethane mixed matrix membranes for carbon dioxide separation, Results in Materials 13 (2022) 100243. https://doi.org/https://doi.org/10.1016/j.rinma.2021.100243

Pacheco, M.J., Vences, L.J., Moreno, H., Pacheco, J.O., Valdivia, R., Hernández, C., 2021. Review: mixed-matrix membranes with CNT for CO2 separation processes. Membranes.

Pan, H., Li, Z., Yang, J., Li, X., Ai, X., Hao, Y., Zhang, H., Dong, L., 2018. The effect of MDI on the structure and mechanical properties of poly(lactic acid) and poly(butylene adipate-co-butylene terephthalate) blends. RSC Adv. 8 (9), 4610–4623. https://doi.org/10.1039/C7RA10745E.

Park, C.H., Tocci, E., Fontananova, E., Bahattab, M.A., Aljlil, S.A., Drioli, E., 2016. Mixed matrix membranes containing functionalized multiwalled carbon nanotubes: mesoscale simulation and experimental approach for optimizing dispersion. J. Membr. Sci. 514, 195–209. https://doi.org/10.1016/j.memsci.2016.04.011.

Rayekan Iranagh, F., Asghari, M., Parnian, M.J., 2020. Dispersion engineering of MWCNT to control structural and gas transport properties of PU mixed matrix membranes. J. Environ. Chem. Eng. 8, (6). https://doi.org/10.1016/j.jece.2020.104493 104493.

Rosenthal, J.J., Hsieh, I.M., Malmali, M.M., 2022. ZSM-5/thermoplastic polyurethane mixed matrix membranes for pervaporation of binary and ternary mixtures of n-Butanol, ethanol, and water. Industrial Eng. Chem. Res. 61 (34), 12764–12775. https://doi.org/10.1021/acs.iecr.2c01794.

Sadeghi, M., Semsarzadeh, M.A., Barikani, M., Ghalei, B., 2011. Study on the morphology and gas permeation property of polyurethane membranes. J. Membr. Sci. 385–386, 76–85. https://doi.org/10.1016/j.memsci.2011.09.024.

Sadeghi, M., Semsarzadeh, M.A., Barikani, M., Pourafshari Chenar, M., 2011. Gas separation properties of polyether-based polyurethane–silica nanocomposite membranes. J. Membr. Sci. 376 (1), 188–195. https://doi.org/10.1016/j.memsci.2011.04.021.

Sadeghi, M., Afarani, H.T., Tarashi, Z., 2015. Preparation and investigation of the gas separation properties of polyurethane-TiO2 nanocomposite membranes. Korean J. Chem. Eng. 32 (1), 97–103. https://doi.org/10.1007/s11814-014-0198-9.

Salahshoori, I., Cacciotti, I., Seyfaee, A., Babapoor, A., 2021. Improvement efficiency of the of poly (ether-block-amide) -Cellulose acetate (Pebax-CA) blend by the addition of nanoparticles (MIL-53 and NH2-MIL-53): a molecular dynamics study. J. Polym. Res. 28 (6), 223. https://doi.org/10.1007/s10965-021-02577-z.

Salahshoori, I., Nasirian, D., Rashidi, N., Hossain, M.K., Hatami, A., Hassanzadeganroudsari, M., 2021. The effect of silica nanoparticles on polysulfone–polyethylene glycol (PSF/PEG) composite membrane on gas separation and rheological properties of nanocomposites. Polym. Bull. 78 (6), 3227–3258. https://doi.org/10.1007/s00289-020-03255-8.

Salahshoori, I., Seyfaee, A., Babapoor, A., Neville, F., Moreno-Atanasio, R., 2021. Evaluation of the effect of silica nanoparticles, temperature and pressure on the performance of PSF/PEG/SiO2 mixed matrix membranes: a molecular dynamics simulation (MD) and design of experiments (DOE) study. J. Mol. Liq. 333,. https://doi.org/10.1016/j.molliq.2021.115957 115957.

Salahshoori, I., Seyfaee, A., Babapoor, A., 2021. Recent advances in synthesis and applications of mixed matrix membranes. Synth. Sinter. 1 (1), 1–27. https://doi.org/10.53063/synsint.2021.116.

Salahshoori, I., Babapoor, A., Seyfaee, A., 2022. Elevated performance of the neat, hybrid and composite membranes by the addition of nanoparticles (ZIF-67): a molecular dynamics study. Polym. Bull. 79 (6), 3595–3630. https://doi.org/10.1007/s00289-021-03673-2.

Salahshoori, I., Jorabchi, M.N., Asghari, M., Ghasemi, S., Wohlrab, S., 2023. Insights into the morphology and gas separation characteristics of methylene diisocyanate (MDI)-functionalized nanoTiO2 polyurethane: quantum mechanics and molecular simulations studies. J. Mater. Res. Technol. 23, 1862–1886. https://doi.org/10.1016/j.jmrt.2023.01.068.

Sazanova, T.S., Smorodin, K.A., Zarubin, D.M., Otvagina, K.V., Maslov, A.A., Markov, A.N., Fukina, D.G., Mochalova, A.E., Mochalov, L.A., Atlaskin, A.A., Vorotyntsev, A.V., 2022. Morphology effect of zinc oxide nanoparticles on the gas separation performance of polyurethane mixed matrix membranes for CO2 recovery from CH4, O2, and N2. Membranes.

Semsarzadeh, M.A., Sadeghi, M., Barikani, M., 2007. The effect of hard segments on the gas separation properties of polyurethane membranes. Iran. Polym. J. (English) 16 (12), 819–827.

Semsarzadeh, M.A., Ghalei, B., Fardi, M., Esmaeeli, M., Vakili, E., 2014. Structural and transport properties of polydimethylsiloxane based polyurethane/silica particles mixed matrix membranes for gas separation. Korean J. Chem. Eng. 31 (5), 841–848. https://doi.org/10.1007/s11814-013-0292-4.

Shamsabadi, A.A., Seidi, F., Salehi, E., Nozari, M., Rahimpour, A., Soroush, M., 2017. Efficient CO2-removal using novel mixed-matrix membranes with modified TiO2 nanoparticles. J. Mater. Chem. A 5 (8), 4011–4025. https://doi.org/10.1039/C6TA09990D.

Shoukat, A., Zubair, M., Uddin, J., Khan, A., Al-Harrasi, A., 2022. Innovative synthesis of non-porous polyurethane membranes with enhanced mechanical, thermal and adsorption properties. Polym. Bull. https://doi.org/10.1007/s00289-022-04383-z.

Sianipar, M., Kim, S.H., Khoiruddin, F., Iskandar, I.G.W., 2017. Functionalized carbon nanotube (CNT) membrane: progress and challenges. RSC Adv. 7 (81), 51175–51198. https://doi.org/10.1039/C7RA08570B.

Sodeifian, G., Raji, M., Asghari, M., Rezakazemi, M., Dashti, A., 2019. Polyurethane-SAPO-34 mixed matrix membrane for CO2/CH4 and CO2/N2 separation. Chin. J. Chem. Eng. 27 (2), 322–334. https://doi.org/10.1016/j.cjche.2018.03.012.

Talakesh, M.M., Sadeghi, M., Chenar, M.P., Khosravi, A., 2012. Gas separation properties of poly(ethylene glycol)/poly(tetramethylene glycol) based polyurethane membranes. J. Membr. Sci. 415–416, 469–477. https://doi.org/10.1016/j.memsci.2012.05.033.

X. Tan, D. Rodrigue, A review on porous polymeric membrane preparation. Part ii: Production techniques with polyethylene, polydimethylsiloxane, polypropylene, polyimide, and polytetrafluoroethylene, Polymers 11(8) (2019) 1310.

Tang, X., Liu, J., Chen, P., Wu, C., Li, X., Pan, Y., Liang, Y., 2023. Effective N-formylation of amines with CO_2 in anaerobic fermentation gas catalyzed by triply synergistic effect of ionic porous organic polymer. ChemCatChem 15 (4). https://doi.org/10.1002/cctc.202201351.

Thür, R., Van Havere, D., Van Velthoven, N., Smolders, S., Lamaire, A., Wieme, J., Van Speybroeck, V., De Vos, D., Vankelecom, I.F. J., 2021. Correlating MOF-808 parameters with mixed-matrix membrane (MMM) CO2 permeation for a more rational MMM development. J. Mater. Chem. A 9 (21), 12782–12796. https://doi.org/10.1039/D0TA10207E.

Torre-Celeizabal, A., Casado-Coterillo, C., Garea, A., 2022. Biopolymer-based mixed matrix membranes (MMMs) for CO2/CH4 separation: experimental and modeling evaluation. Membranes.

Valizadeh, K., Heydarinasab, A., Hosseini, S.S., Bazgir, S., 2022. Fabrication of modified PVDF membrane in the presence of PVI polymer and evaluation of its performance in the filtration process. J. Ind. Eng. Chem. 106, 411–428. https://doi.org/10.1016/j.jiec.2021.11.016.

van Essen, M., van den Akker, L., Thür, R., Houben, M., Vankelecom, I.F.J., Borneman, Z., Nijmeijer, K., 2021. The influence of pore aperture, volume and functionality of isoreticular gmelinite zeolitic imidazolate frameworks on the mixed gas CO2/N2 and CO2/CH4 separation performance in mixed matrix membranes. Sep. Purif. Technol. 260,. https://doi.org/10.1016/j.seppur.2020.118103 118103.

Vinoba, M., Bhagiyalakshmi, M., Alqaheem, Y., Alomair, A.A., Pérez, A., Rana, M.S., 2017. Recent progress of fillers in mixed matrix membranes for CO2 separation: a review. Sep. Purif. Technol. 188, 431–450. https://doi.org/10.1016/j.seppur.2017.07.051.

Wang, X., Ding, X., Zhao, H., Fu, J., Xin, Q., Zhang, Y., 2020. Pebax-based mixed matrix membranes containing hollow polypyrrole nanospheres with mesoporous shells for enhanced gas permeation performance. J. Membr. Sci. 602,. https://doi.org/10.1016/j.memsci.2020.117968 117968.

Wang, T., Yang, C.-H., Man, C.-L., Wu, L.-G., Xue, W.-L., Shen, J.-N., Van der Bruggen, B., Yi, Z., 2017. Enhanced separation performance for CO2 gas of mixed-matrix membranes incorporated with TiO2/graphene oxide: synergistic effect of graphene oxide and small TiO2 particles on gas permeability of membranes. Ind. Eng. Chem. Res. 56 (31), 8981–8990. https://doi.org/10.1021/acs.iecr.7b02191.

Wu, R., Tan, Y., Meng, F., Zhang, Y., Huang, Y., 2022. PVDF/MAF-4 composite membrane for high flux and scaling-resistant membrane distillation. Desalination 540,. https://doi.org/10.1016/j.desal.2022.116013 116013.

Xin, Q., Wu, H., Jiang, Z., Li, Y., Wang, S., Li, Q., Li, X., Lu, X., Cao, X., Yang, J., 2014. SPEEK/amine-functionalized TiO2 submicrospheres mixed matrix membranes for CO2 separation. J. Membr. Sci. 467, 23–35. https://doi.org/10.1016/j.memsci.2014.04.048.

Zagho, M.M., Hassan, M.K., Khraisheh, M., Al-Maadeed, M.A.A., Nazarenko, S., 2021. A review on recent advances in CO2 separation using zeolite and zeolite-like materials as adsorbents and fillers in mixed matrix membranes (MMMs). Chem. Eng. J. Adv. 6,. https://doi.org/10.1016/j.ceja.2021.100091 100091.

Zhang, K., Deng, Q., Luo, J., Gong, C., Chen, Z., Zhong, W., Wang, H., 2021. Multifunctional Ag(I)/CAAA-Amidphos complex-catalyzed asymmetric [3 + 2] cycloaddition of α-substituted acrylamides. ACS Catal. 11 (9), 5100–5107. https://doi.org/10.1021/acscatal.1c00913.

Zhang, J., Xin, Q., Li, X., Yun, M., Xu, R., Wang, S., Li, Y., Lin, L., Ding, X., Ye, H., Zhang, Y., 2019. Mixed matrix membranes comprising aminosilane-functionalized graphene oxide for enhanced CO2 separation. J. Membr. Sci. 570–571, 343–354. https://doi.org/10.1016/j.memsci.2018.10.075.

Zhao, Y., Wu, M., Guo, Y., Mamrol, N., Yang, X., Gao, C., Van der Bruggen, B., 2021. Metal-organic framework based membranes for selective separation of target ions. J. Membr. Sci. 634,. https://doi.org/10.1016/j.memsci.2021.119407 119407.

Zhu, H., Wang, L., Jie, X., Liu, D., Cao, Y., 2016. Improved interfacial affinity and CO_2 separation performance of asymmetric mixed matrix membranes by incorporating postmodified MIL-53 (Al). ACS Appl. Mater. Interfaces 8 (34), 22696–22704. https://doi.org/10.1021/acsami.6b07686.

Zhu, H., Yuan, J., Zhao, J., Liu, G., Jin, W., 2019. Enhanced CO2/N2 separation performance by using dopamine/polyethyleneimine-grafted TiO2 nanoparticles filled PEBA mixed-matrix membranes. Sep. Purif. Technol. 214, 78–86. https://doi.org/10.1016/j.seppur.2018.02.020.